

LA-UR--87-3617

DE88 001800

TITLE: CHEMICAL SHORT-RANGE ORDER IN DENSE RANDOM PACKED MODELS

AUTHOR(S): C. K. Saw and R. B. Schwarz

SUBMITTED TO Int'l. Conf. of Solid State Amorphizing Transformations,  
Los Alamos, NM, August 10-13, 1987. Proceeding to be  
published in the J. of Less Common Metals.

## DISCLAIMER

This report was prepared as an account of work sponsored by an agency of the United States Government. Neither the United States Government nor any agency thereof, nor any of their employees, makes any warranty, express or implied, or assumes any legal liability or responsibility for the accuracy, completeness, or usefulness of any information, apparatus, product, or process disclosed, or represents that its use would not infringe privately owned rights. Reference herein to any specific commercial product, process, or service by trade name, trademark, manufacturer, or otherwise does not necessarily constitute or imply its endorsement, recommendation, or favoring by the United States Government or any agency thereof. The views and opinions of authors expressed herein do not necessarily state or reflect those of the United States Government or any agency thereof.

By acceptance of this article, the publisher recognizes that the U.S. Government retains a nonexclusive, royalty-free license to publish or reproduce the published form of this contribution or to allow others to do so, for U.S. Government purposes.

The Los Alamos National Laboratory requests that the publisher identify this article as work performed under the auspices of the U.S. Department of Energy.

**MASTER** **Los Alamos** Los Alamos National Laboratory  
Los Alamos, New Mexico 87545

CHEMICAL SHORT-RANGE ORDER IN  
DENSE RANDOM PACKED MODELS<sup>+</sup>

C. K. Saw<sup>\*</sup> and R. B. Schwarz<sup>\*\*</sup>

<sup>\*</sup>Hoechst Celanese Corporation  
86, Morris Avenue, Summit, NJ 07901,

<sup>\*\*</sup>Center for Materials Science  
Los Alamos National Laboratory  
Los Alamos, NM 87545

SUMMARY

A dense random packed model of an amorphous alloy was used to calculate the total and partial reduced radial distribution functions, the Bhathia-Thorton number-concentration fluctuations, and the number-concentration interference functions. The model was applied to amorphous Ni<sub>35</sub>Ti<sub>65</sub> using atomic radii of 1.10 and 1.58 Å<sup>-1</sup> for nickel and zirconium, respectively. Chemical short range order was included in the model by permuting nickel-zirconium nearest-neighbors atoms pairs in response to a decrease in the alloy's enthalpy. The permutations were found to decrease in the Warren-Cowley order parameter from zero to -0.38, in good agreement with the measured value of -0.40. The increase in chemical short range order is accompanied by the appearance of a peak in the partial interference function  $I_{N_1-N_1}(K)$  at  $K = 1.9 \text{ Å}^{-1}$  which is

---

<sup>+</sup> Part of this work was performed while both authors were at the Argonne National Laboratory, Argonne, Illinois. Work supported in part by the United States Department of Energy.

---

Paper submitted to the Int'l. Conf. of Solid State Amorphizing Transformations, Los Alamos National Laboratory, August 10-13, 1987. Proceeding to be published in the J. of the Less Common Metals. (R. B. Schwarz and W. L. Johnson, eds.)

similar in form, and is located at the same K value, as the so-called "pre-peak" commonly observed in rapidly quenched binary amorphous alloys containing Ni. The increase in chemical short range order and the prepeak in  $I_{\text{Ni-Ni}}(K)$  are tentatively attributed to the formation of double tetrahedra with three zirconium atoms at the base and two nickel atoms at the apexes.

## 1. INTRODUCTION

In recent years, scattering techniques [1] have improved significantly allowing the derivation of more accurate partial correlation functions for amorphous alloys. The interpretation of these measurements requires modeling the atomic structure with the inclusion of effects such as chemical short range order (CSRO). Dense Random Packed (DRP) models have been extensively used to simulate the structure of amorphous alloys [2] and, in general, good agreement has been found between the calculated and measured radial distribution functions. However, the fixed nature of the DRP model does not lend itself to the simulation of dynamic processes involving atomic rearrangements. For this type of problem the molecular dynamic simulations are more appropriate except that the simulation of events in real time often requires excessive computational time.

The most widely used computer code for DRP models is based on Bennett's "global" algorithm [3]. Detailed investigations of this model [4,5] established that the criteria has various deficiencies: (a) the pair correlation functions derived from this model has spatial anisotropy; (b) the smaller atoms tend to drift towards the center of the cluster; and (c) the relaxation of the structure to eliminate holes created each time an

atom is added to the cluster requires excessive computational time. A better and more efficient model was suggested by Sharma et al. [6] which is based on the collapsing of a loosely packed amorphous atomic structure. This model has no spatial anisotropy in the unrelaxed or in the relaxed structures. Furthermore, the computational time is relatively short.

In an earlier paper [7] we reported the results of modeling calculations using Sharma's DRP model. For all calculations in which either the atomic size ratio or the relative strength of the interatomic forces were changed we observed that the Warren-Cowley short-range order parameter,  $\alpha_w$ , remained close to zero. This means that the unperturbed model is quite appropriate for further investigations involving short range order. We then developed a technique [8] to simulate the chemical short range expected to develop in binary amorphous alloys with large negative heats of mixing during their rapid solidification from the melt. In essence the technique introduces permutations between near-neighbor atoms whenever such a change decreases the alloy's enthalpy. The calculations were performed for amorphous  $\text{Ni}_{35}\text{Zr}_{65}$ , for which there exist detailed diffraction data [9,10,11]. The atomic permutations were shown to (a) improve the agreement between the calculated and measured Bathia-Thorton pair correlation functions and (b) decrease the value of  $\alpha_w$  to -0.38, in excellent agreement with the measured value of -0.40.

In this paper we report calculations of the partial interference functions of  $\text{Ni}_{35}\text{Zr}_{65}$  as a function of the degree of chemical short range order introduced in the model. We observe that an increase in the number of atomic permutations causes an increase in the magnitude of the first peak in  $S_{cc}(K)$  and a shift of this peak towards lower wavenumber,  $K$ . The

structure factor  $I_{N1-N1}(K)$  also shows a clear increase in the magnitude of its first peak, at  $K = 1.9 \text{ \AA}^{-1}$ , and a shift of this peak towards lower  $K$  values. We propose that this peak is the so-called "pre peak" that has been reported in the  $I_{N1-N1}(K)$  functions of various amorphous binary alloys between nickel and an early transition metal.

## 2. CALCULATIONS

### 2.1 Atomic Distribution Functions

The density distribution function,  $g(r)$ , can be obtained from the DRP model by simply counting the number of atoms in the radial shell between  $r$  and  $r+dr$  and dividing by the volume of the shell. The reduced radial distribution function of a monoatomic system,  $G(r)$ , is defined as.

$$G(r) = 4\pi r(\rho(r) - \rho_0) \quad (1)$$

where  $\rho_0$  is the average density. For a multicomponent system, the partial reduced distribution functions are defined as,

$$G_{ij}(r) = 4\pi r(\rho_{ij}(r) - \rho_0) \quad (2)$$

where  $i, j$  denote the atomic species, and  $c_j$  is the concentration of the  $j$  atoms.

### 2.2 Number Concentration Fluctuations

A binary system has three independent partial reduced distribution functions,  $G_{11}$ ,  $G_{12}$ , and  $G_{22}$ . For the study of chemical ordering it is convenient to work with linear combinations of the distribution functions. The Bathia-Thorton concentration fluctuations are defined as,

$$G_{NN}(r) = c_1^2 G_{11}(r) + c_2^2 G_{22}(r) + 2c_1 c_2 G_{12}(r) \quad (3)$$

$$G_{NC}(r) = c_1 c_2 ([c_1 G_{11}(r) + c_2 G_{12}(r)] - [c_1 G_{21}(r) + c_2 G_{22}(r)]) \quad (4)$$

$$G_{CC}(r) = c_1 c_2 [G_{11}(r) + G_{22}(r) - 2G_{21}(r)] \quad (5)$$

The  $G_{NN}(r)$  correlation describes the topological distribution;  $G_{NC}(r)$  is proportional to the size effect; and  $G_{CC}(r)$  describes the chemical ordering.

The Warren chemical short range order parameter,  $\alpha_w$ , is defined as,

$$\alpha_w = \frac{c_2(Z_{11} - Z_{21}) + c_1(Z_{22} + Z_{12})}{c_2(Z_{11} + Z_{12}) + c_1(Z_{21} + Z_{22})} \quad (6)$$

where  $Z_{ij}$  are the coordination numbers defined as,

$$Z_{ij} = \int_0^{r_{\min}} 4\pi r^2 \rho_{ij}(r) dr \quad (7)$$

and the integral extends from zero to the first minima in  $r$ .

### 2.3 Number-Concentration Interference Functions

The partial interference functions (or structure factors) are derived from a Fourier transformation of the reduced partial correlation functions  $G_{ij}(r)$ ,

$$I_{ij}(K) = 1 + \frac{1}{K} \int_0^\infty G_{ij}(r) \sin(Kr) dr \quad (8)$$

The three number-concentration interference functions of a binary alloy are:

$$S_{NN}(K) = c_1^2 I_{11}(K) + c_2^2 I_{22}(K) + c_1 c_2 I_{12}(K) \quad (9)$$

$$S_{NC}(K) = c_1 c_2 ([c_1 I_{11}(K) + c_2 I_{12}(K)] - [c_1 I_{21}(K) + c_2 I_{22}(K)]) \quad (10)$$

$$S_{CC}(K) = c_1 c_2 (1 + c_1 c_2 [I_{11}(K) + I_{22}(K) - 2I_{12}(K)]) \quad (11)$$

A more detailed description of these functions has been given by Wagner [12].

### 3. MODELING RESULTS

A DRP model for  $Ni_{35}Zr_{65}$  was constructed using approximately 3400 atoms, as described previously [6-8]. The atomic radii used in the model were 1.10 Å for nickel and 1.58 Å for Zr. The as-constructed DRP model has no chemical short range order (CSRO) as verified by a zero value for the calculated  $\alpha_v$  parameter. CSRO was introduced into the model in a discrete manner in the following way. The computer code selects at random a pair of dissimilar nearest-neighbor atoms (Ni and Zr in this case) and defines a microensemble of the atomic array consisting of the two atoms selected and all their nearest neighbours. The code then permutes the two atoms chosen if this causes a decrease in the enthalpy of the microensemble. For this, the computer assumes that the enthalpy of a Ni-Zr bond is lower than that of Ni-Ni or a Zr-Zr bond. This assumption reflects the large negative heat of mixing of Ni and Zr (-71 KJ/g-at for the equimolar intermetallic compound [13]). This process is repeated for all the Ni-Zr pairs in the model. The calculation does not include entropy effects and thus it is strictly a zero-temperature simulation. This is a reasonable approximation since the enthalpy decrease per permutation is several eV, large compared to kT. Following the completion of the "permutation" routine, the code relaxes the DRP model by minimizing a Keating elastic energy sum which was modified to include only central

forces [4]. The "permutation" routine can be applied repeatedly, causing a further increase in the CSRO of the DRP model. However, after a few applications of the "permutation" routine the value of  $\alpha_w$  reaches a saturation. [8] This is because the local increase in CSRO obtained by permuting two atoms of a given microensemble is later destroyed by the permutations in adjacent, and partially overlapping, microensembles.

The serrated curves in Fig. 1 show the calculated total reduced radial distribution,  $G(r)$ , and the Bathia-Thorton number-concentration fluctuations before (left) and after (right) the first application of the "permutation" routine. The smooth curves are experimental data of Wagner and Lee [10,14]. In general, there is a good agreement between the model calculations and the measurements. The most significant change that occurs as the result of the "permutation" routine is observed in the first double peak of  $G(r)$  and  $G_{NN}(r)$ , where there is an improvement in the fit between the calculated and measured distributions in the regime 2 to 4 Å. The "permutation" routine causes a change in the value of  $\alpha_w$  from 0 to -0.38, indicating that there is an increase in the alloy's CSRO. A second and third application of the "permutation" routine causes a further increase in the degree of CSRO, as verified by a decrease in  $\alpha_w$ , [8] but this does not improve significantly the fit of the model calculations to the data.

Figure 2 shows the three partial reduced distribution functions before (left) and after (right) the first application of the "permutation" routine. No significant changes can be seen in either  $G_{Ni-Zr}(r)$  nor  $G_{Zr-Zr}(r)$ .  $G_{Ni-Ni}(r)$  shows a small peak at  $r = 4.1$  Å (indicated by the arrow). However, this peak is not significantly larger than the



background noise. We will show below that this peak is indeed caused by the CSRO introduced in the amorphous structure by the "permutation" routine.

Even though the addition of CSRO does not change significantly the distribution functions in real space, it gives clear signatures on the structure factors in K-space. Figure 3 shows the structure factors,  $I_{ij}(K)$ , as a function of wavenumber K. The labels a, b, c, and d denote 0, 1, 2, and 3 applications of the "permutation" routine, respectively. These curves clearly show that the CSRO causes the appearance of a peak in  $I_{Ni-Ni}(K)$  near  $K = 1.9 \text{ \AA}^{-1}$ . With increasing number of applications of the "permutation" routine the peak increases slightly in magnitude and shifts towards lower K values (see table 1). The increase in CSRO causes no apparent changes in the other two partial interference functions.

Figure 4 shows the number-concentration interference functions,  $S_{ij}(K)$ , calculated from the model according to equations (8)-(11). The most significant change as the result of the increase in CSRO occurs in the first peak of  $S_{CC}(K)$ . This peak not only increases in intensity, but also shifts from approximately  $2.2 \text{ \AA}^{-1}$  in curve (a) ( $\alpha_w = 0$ ) to  $1.95 \text{ \AA}^{-1}$  in curve (d) ( $\alpha_w = -0.6$ ).  $S_{NN}(K)$  and  $S_{NC}(K)$  show no significant changes as the result of the increase in CSRO.

Debye's formula can be used to deduce the interatomic distance, D, that gives rise to the pre-peak in  $I_{Ni-Ni}(K)$  at  $K=1.9 \text{ \AA}^{-1}$ :

$$D = \pi \sqrt{6} / K = 4.05 \text{ \AA} \quad (12)$$

This distance corresponds to that of the small peak in  $G_{Ni-Ni}(r)$  indicated by the arrow in figure 2.

## 4 DISCUSSION

The appearance of a pre-peak in the  $I_{\text{Ni-Ni}}(K)$  interference function of amorphous alloys containing Ni is an ubiquitous phenomena which has been well documented by neutron diffraction measurements. It has been reported in rapidly quenched foils of  $\text{Ni}_{40}\text{Ti}_{60}$  [15] and  $\text{Ni}_{50}\text{Zr}_{50}$  [16] and in a sputter-deposited foil of  $\text{Ni}_{58}\text{V}_{42}$  [17]. Figure 5 shows the measurements of Hayashi et al. [16] in rapidly quenched amorphous  $\text{Ni}_{50}\text{Zr}_{50}$ . The prepeak in  $I_{\text{Ni-Ni}}(K)$  at  $K = 1.9 \text{ \AA}^{-1}$  is quite similar to that which develops in the  $I_{\text{Ni-Ni}}(K)$  curves for the DRP model (Fig. 3) following the application of the "permutation" routine. We thus conclude that the "pre-peak" is caused by CSRO that occurs when Ni-T atoms pairs in the amorphous alloy (T stands for an earlier transition metal having a large negative heat of mixing with nickel) are allowed to permute so as to increase the number of Ni-T bonds at the expense of Ni-Ni and T-T bonds. This simple type of ordering does not involve long range chemical diffusion and is most likely to occur during the rapid solidification of the molten alloy. The observation of the pre-peak in sputtered samples [16], where the equivalent cooling rates are extremely high, suggest that this simple type of ordering is difficult to avoid during rapid solidification. It would be thus interesting to investigate amorphous alloys prepared by mechanical alloying [18], where the equivalent fictive temperature seems to be is very high.

The interpretation of the CSRO in terms of atomic clusters requires a detailed statistical analysis of DRP model. However, the signatures of the CSRO are more pronounced in  $I_{\text{Ni-Ni}}(K)$  and  $S_{\text{CC}}(K)$  than in the real-

space function  $G_{\text{Ni-Ni}}(r)$ , and this makes the analysis difficult. Our preliminary statistical analysis suggest that the atomic clusters responsible for the appearance of the "pre-peak" in  $I_{\text{Ni-Ni}}(K)$ , are double tetrahedra consisting of three zirconium atoms at the base with nickel atoms on top and bottom. The Ni-Ni separation for these arrangements is close to  $4.1 \text{ \AA}^{-1}$ . More detailed statistical calculations will be derived from calculations using larger DRP models.

## FIGURE CAPTIONS

- Fig. 1. Broken curves are the calculated total reduced radial distribution,  $G(r)$ , and the Bathia-Thornton number-concentration fluctuation, before (left) and after (right) the first application of the "permutation" routine to the dense random packed model. The smooth curves are the measurements of Wagner and Lee in rapidly quenched amorphous  $\text{Ni}_{35}\text{Zr}_{65}$ .
- Fig. 2. Partial reduced distribution functions before (left) and after (right) the first application of the "permutation" routine to the dense random packed model. The arrow denotes a small peak in  $G_{\text{Ni-Ni}}(r)$  at  $r=4.1 \text{ \AA}$ .
- Fig. 3. Partial atomic structure functions for the dense random packed model. The labels a, b, c, and d denote 0, 1, 2, and 3 successive applications of the "permutation" routine. Notice the appearance of a peak in  $I_{\text{Ni-Ni}}(K)$  at  $K=1.9 \text{ \AA}^{-1}$ .
- Fig. 4. Number-concentration interference functions for the dense random packed model. The labels a, b, c, and d denote 0, 1, 2, and 3 successive applications of the "permutation" routine. Notice the increase in the first peak in  $S_{\text{CC}}(K)$  near  $K=2 \text{ \AA}^{-1}$ .
- Fig. 5. Partial atomic structure factors for rapidly quenched amorphous  $\text{Ni}_{50}\text{Zr}_{50}$  measured by pulse neutron scattering (after Hayashi et al., [16]).

## REFERENCES

1. See, for example, C.N.J. Wagner, J. Non-Cryst. Solids 31 (1978).
2. G.S. Cargill, Solid State Phys., 30 (Academic Press, New York, 1975).
3. C.H. Bennett, J. Appl. Phys. 43 (1972) 2727.
4. D.S. Boudreaux and J.M. Gregor, J. of Appl. Phys. 48 (1977) 152.
5. R. Alben, G.S. Cargill III and J. Wenzel, Phy. Rev. B, 13 (1976) 835.
6. Y.P. Sharma, C.K. Saw and S.J. Pickart, J. on Non-Cryst. Solids, 41 (1980) 287.
7. C.K. Saw and J. Faber Jr., J. of Non-Cryst. Solids 75 (1985) 347-354.
8. C.K. Saw and R.B. Schwarz, J. of Non-Cryst. Solids 75 (1985) 355.
9. S. Lefebvre, A. Quivy, J. Bigot, Y. Calvayrac and R. Bellissent, J. Phys. F (Met. Phys.) 15 (1985) L99.
10. C.N.J. Wagner and D. Lee, J. Phys. (Paris) 41 (1980) C242.
11. A. Lee, G. Etherington and C.N.J. Wagner, J. Non-Cryst. Solids 61&62 (1984) 349.
12. C.N.J. Wagner, "Atomic Energy Review", suppl 1 (1981) 101
13. A. R. Miedema, Philips Technical Review, 36 (1976) 217.
14. After the completion of this work, we became aware of a more recent set of experimental data by Prof. C.N.J Wagner. Even though the two sets of data have minor differences, these refinements do not affect the present discussion.
15. T. Fukunaga, N. Watanabe and K. Suzuki, J. of Non-Crystalline Solids 61&62 (1984) 343.
16. N. Hayashi, T. Fukunaga, N. Watanabe and K. Suzuki, KENS report-V,

National Laboratory for High Energy Physics, Ibaraki-ken, Japan,  
1984, p.21.

17. T. Fukunaga, S. Urai, N. Hayashi, N. Watanabe and K. Suzuki, KENS  
report-V, National Laboratory for High Energy Physics, Ibaraki-ken,  
Japan, 1984, p.18 and p.40.
18. R. B. Schwarz, R. R. Petrich and C. K. Saw, J. of Non-Crystalline  
Solids 76 (1985) 281.

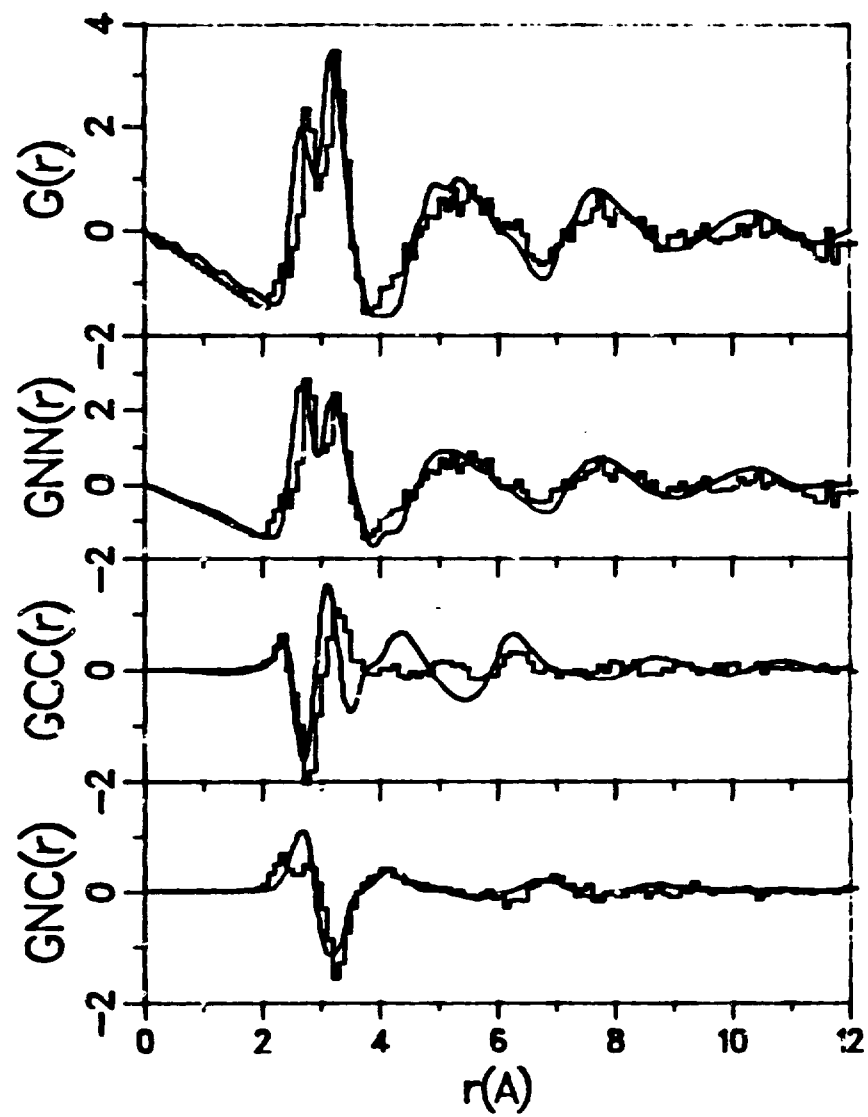
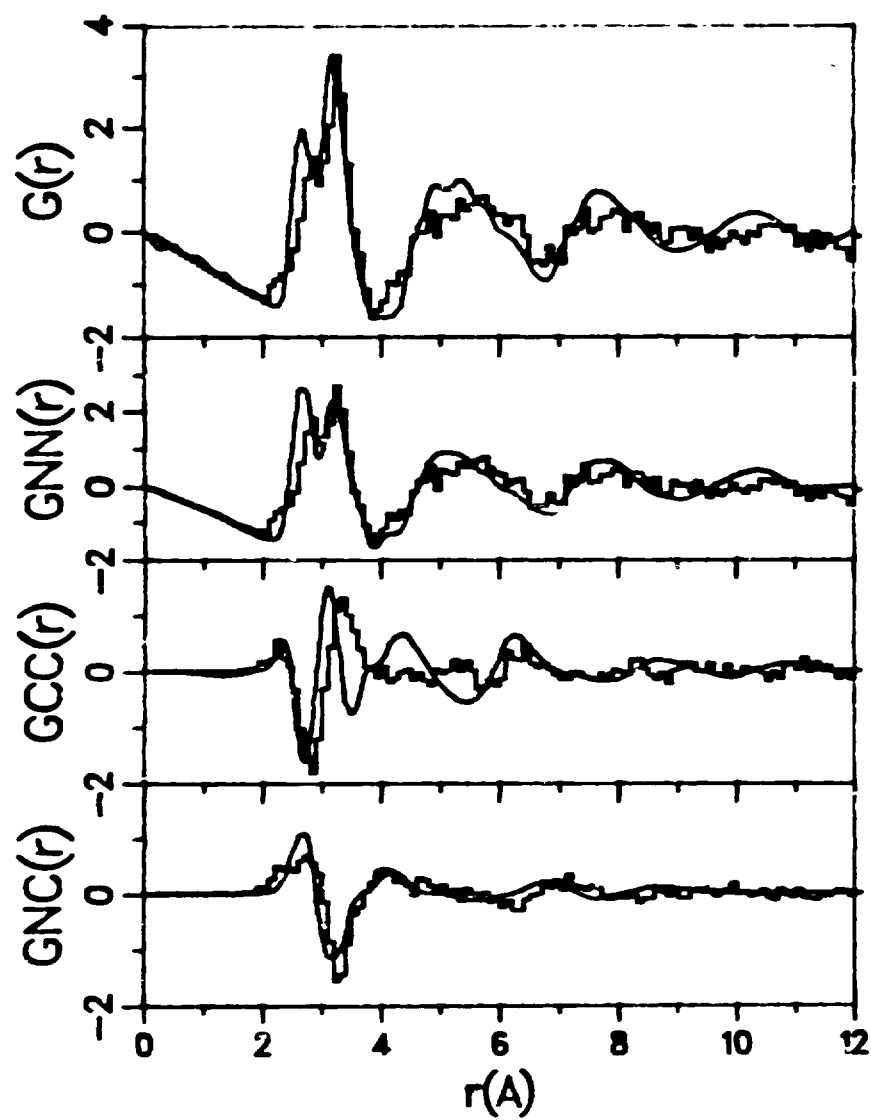


Fig. 1

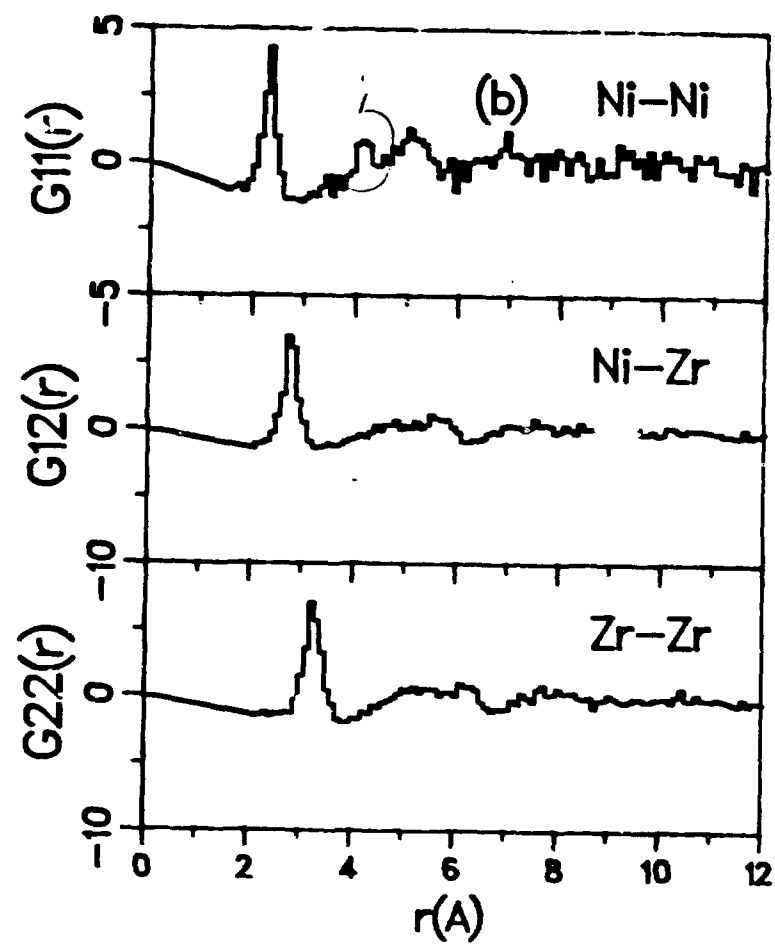
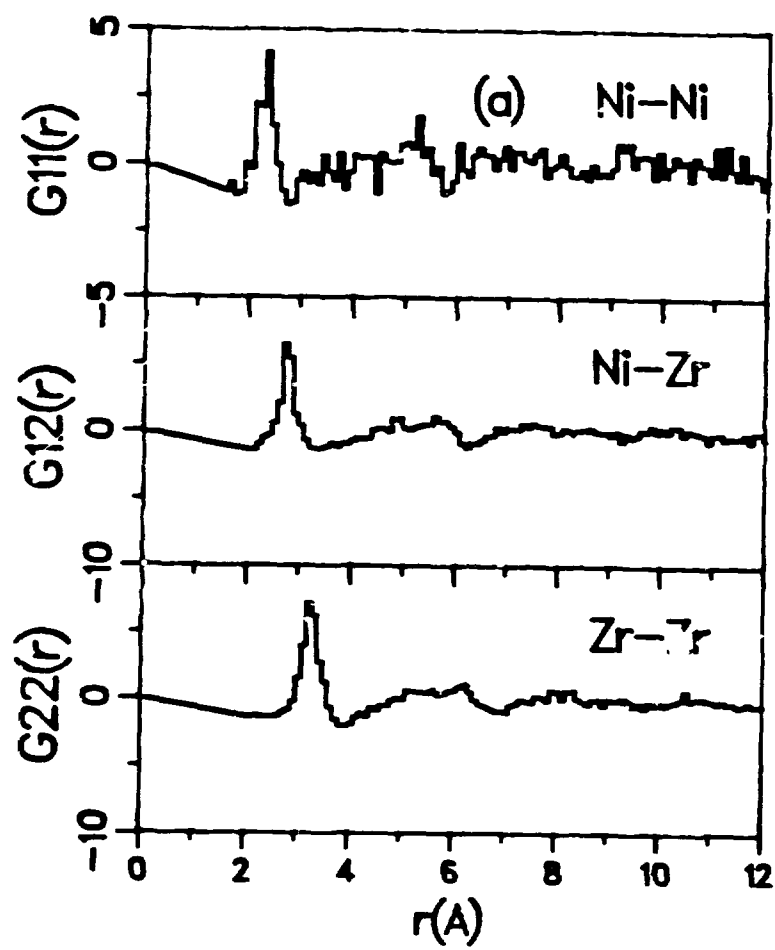


Fig. 2



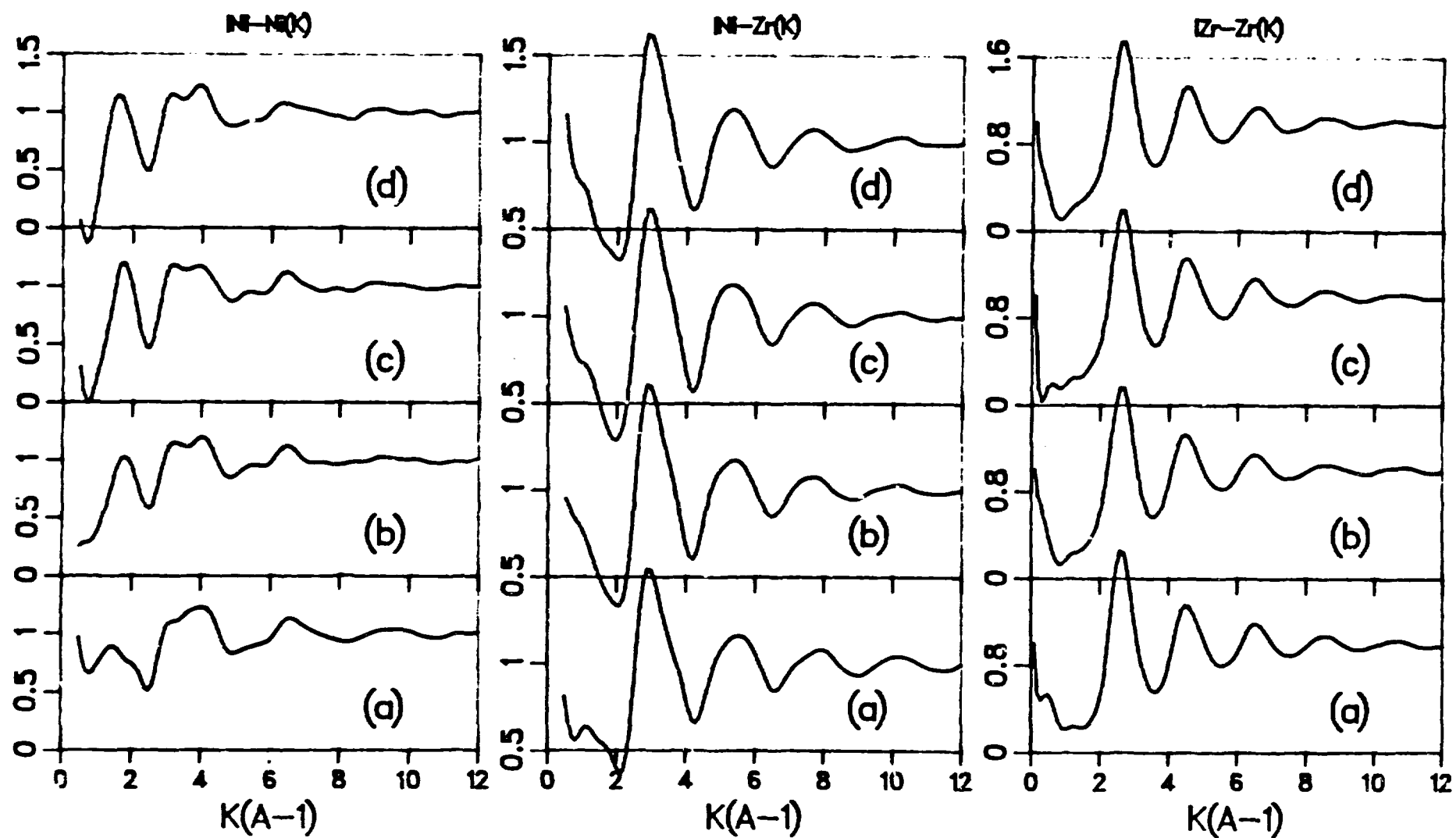


Fig. 3

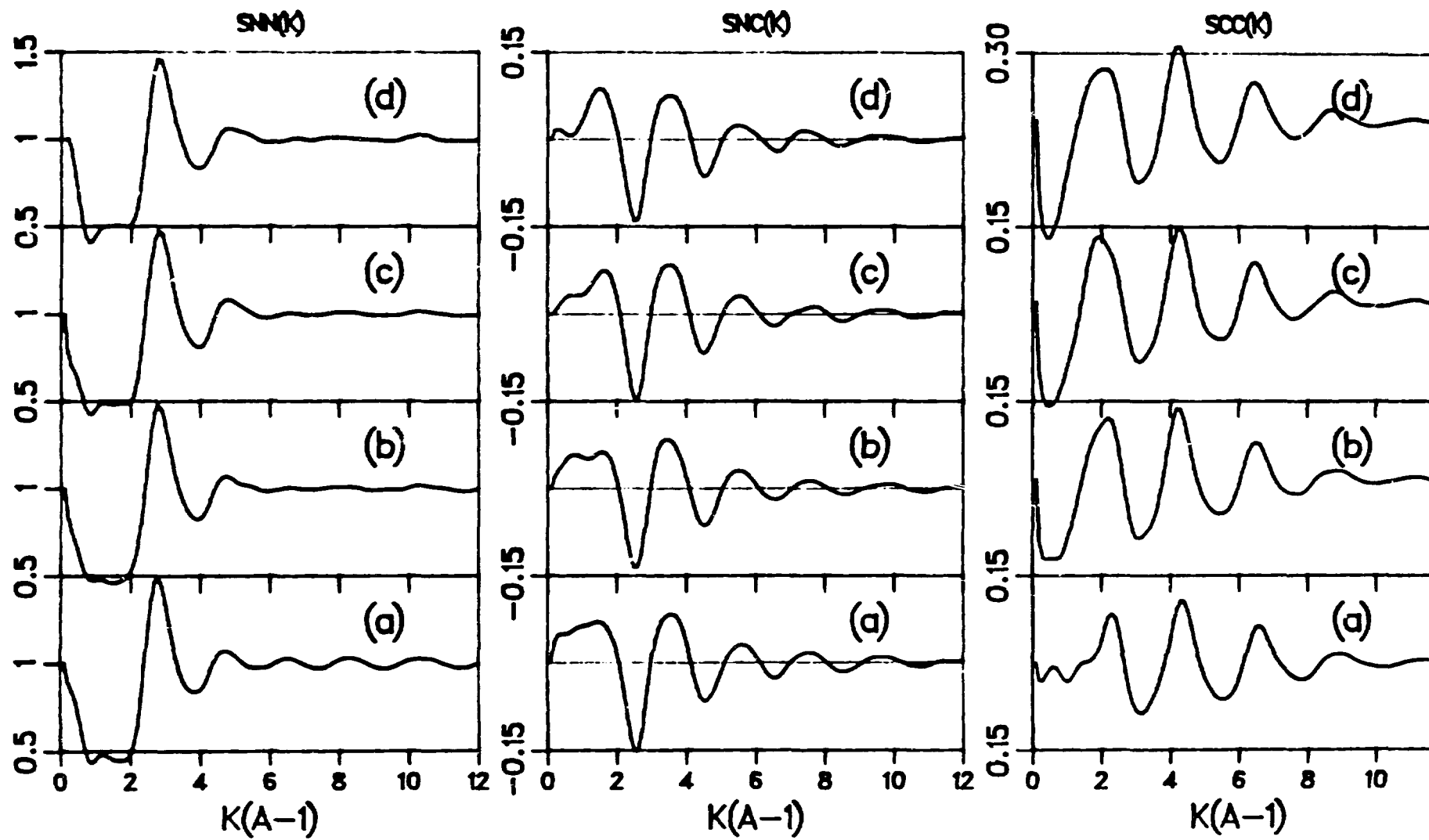


Fig. 4

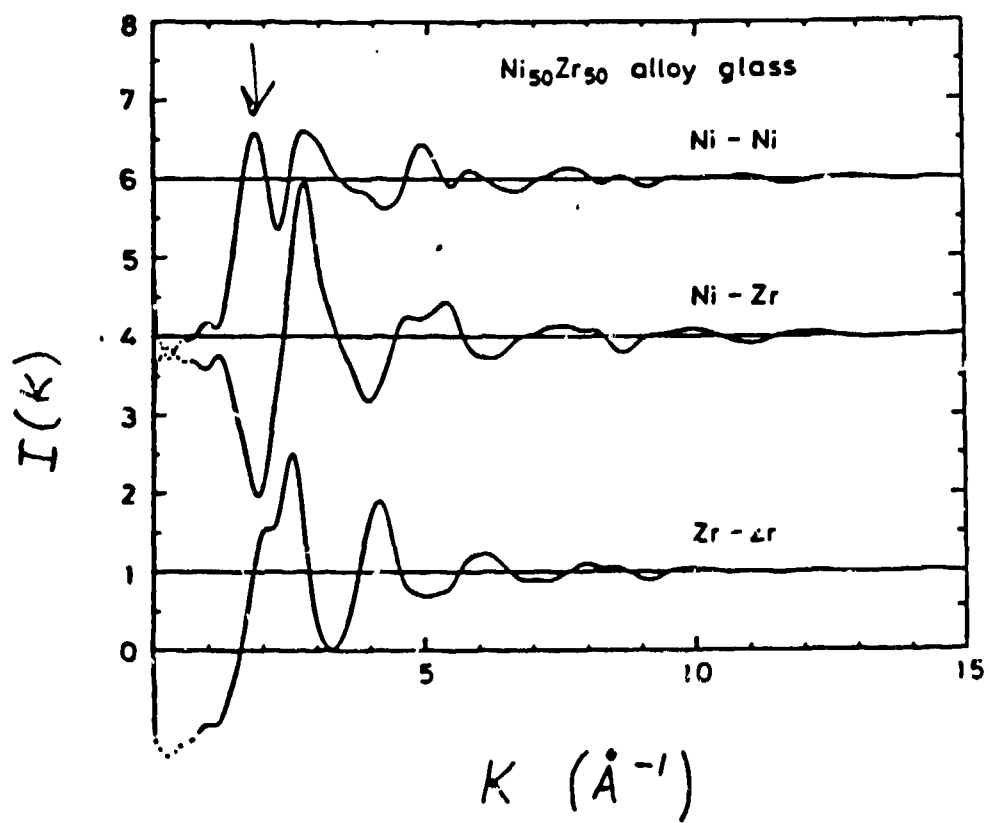


Fig. 5